J|A|C|S
ARTICLES
Published on Web 02/13/2003

Conformational Flexibility of the Group B Meningococcal Polysaccharide in Solution

Terry J. Henderson,*,† Richard M. Venable,‡ and William Egan‡

Contribution of the Edgewood Chemical - Biological Forensic Analytical Center, Battelle Memorial Institute Edgewood Operations, 1204 Technology Drive, Aberdeen, Maryland 21001 and the Laboratory of Biophysics, Center for Biologics Evaluation and Research, Food and Drug Administration, 1401 Rockville Pike, Rockville, Maryland 20852.

Received July 23, 2002; Revised Manuscript Received November 15, 2002; E-mail: txhender@sbccom.apgea.army.mil

Abstract: To elucidate the role of secondary structure in the immune response against α(2→8)-linked polysialic acid, the capsular polysaccharide of Group B meningococci, we have investigated its solution dynamics by using specific models of molecular motion and hydrodynamic modeling to interpret experimental NMR data. $^{13}C-\{^1H\}$ NMR relaxation times and steady-state NOE enhancements were measured for two aqueous solutions of α(2→8)-linked sialic acid polysaccharides. Each contained a unique distribution of polysaccharide chain lengths, with average lengths estimated at 40 or 400 residues. Models for rigid molecule tumbling, including two based on helical conformations proposed for the polysaccharide,[31] could not explain the NMR measurements. In general for these helices, the correlation times for their overall tumbling that best account for the NMR data correspond to polysaccharide chains between 9 and 18 residues in length, far short of the average lengths estimated for either solution. The effects of internal motions incorporated into these helices was modeled with an effective correlation time representing helix tumbling as well as internal motion. This modeling demonstrated that even with extreme amounts of internal motion, "flexible helices" of 25 residues or more still could not produce the NMR measurements. All data are consistent with internal and segmental motions dominating the nuclear magnetic relaxation of the polysaccharide and not molecular tumbling. Statistical distributions of correlation times have been found specifically for the pyranose rings, linkage groups, and methoxy groups that can account for the measured relaxation times and NOE enhancements. The distributions suggest that considerable flexibility attends the polysaccharide in solution, and the ranges of motional frequencies for the linkage groups and pyranose rings are comparable. We conclude that the Group B meningococcal polysaccharide is a random coil chain in solution, and therefore, does not have antigenic epitopes dependent upon a rigid, ordered conformation.

Introduction

Of the 12 known encapsulated serogroups of *Neisseria meningitidis*, the majority of serious invasive diseases—meningitidis and septicemia—are caused by only three, viz., A, B, and C, with B and C currently being the most prevalent disease isolates in the United States.[1,2] Vaccines against the A and C serogroup, consisting of purified capsular polysaccharides from the homologous organisms,[1,3] are licensed in the United States and other countries.[3] A similar polysaccharide-based vaccine against the B serogroup does not exist[1,2] because its capsular polysaccharide is poorly immunogenic in humans.[4] This poor immunogenicity has been attributed to a similarity to self-antigens,[5−9] particularly the neural cell adhesion molecules (N-CAMs).

The Groups B and C polysaccharides are respectively, α-(2→8)- and α(2→9)-linked homopolymers of sialic acid.[10] The Group C polysaccharide is generally O-acetylated,[10] although nonacetylated variants exist.[11] The capsule of the *Escherichia coli* K92 organism is also a homopolymer of sialic acid, consisting of alternating α(2→8) and α(2→9) linkages.[12] Antibodies elicited against the purified K92 polysaccharide cross react with the Group C meningococcal polysaccharide but not its Group B counterpart,[13] a response consistent with the hypothesis that the poor immunogenicity of the Group B

† Battelle Memorial Institute Edgewood Operations.
‡ Food and Drug Administration.

(1) Zollinger, W. D. *New Generation Vaccines*, 2nd ed.; Marcel Dekker: New York, 1997; pp 469−488.
(2) Frasch, C. E. *Meningococcal Disease*; John Wiley and Sons: New York, 1995; pp 245−283.
(3) Frasch, C. E. *Bacterial Vaccines*; Alan R. Liss, Inc., New York, 1990; pp 123−145.
(4) Wyle, F. A.; Artenstein, M. S.; Brant, B. L.; Tramont, E. C.; Kasper, D. L.; Alteri, P. L.; Lowenthal, P. *J. Infect. Dis.* **1972**, *126*, 514−522.
(5) Finne, J.; Leinonen, M.; Mäkela, P. H. *Lancet* **1983**, *2*, 355−357.
(6) Hayrinen, J.; Jennings, H.; Raff, H. V.; Rougon, G.; Hanai, N.; Gerardy-Schahn, R.; Finne, J. *Infect. Dis.* **1995**, *171*, 1481−1490.
(7) Rutishauser, U.; Acheson, A.; Hall, A. K.; Mann, D. M.; Sunshine, J. *Science* **1988**, *240*, 53−57.
(8) Brandley, B. K.; Swiedler, S. J.; Robbins, P. W. *Cell* **1990**, *63*, 861−863.
(9) Corral, L.; Singer, M. S.; Macher, B. A.; Rosen, S. D. *Biochem. Biophys. Res. Commun.* **1990**, *172*, 1349−1356.
(10) Bhattacharjee, A. K.; Jennings, H. J.; Kenney, C. P.; Martin, A.; Smith, I. C. P. *J. Biol. Chem.* **1975**, *250*, 1926−1932.
(11) Appicella, M. A. *J. Infect. Dis.* **1972**, *129*, 147−153.
(12) Egan, W.; Liu, T.-Y.; Dorow, D.; Cohen, J. S.; Robbins, J. D.; Gotschlich, E. C.; Robbins, J. B. *Biochemistry* **1977**, *16*, 3687−3692.
(13) Robbins, J. B.; Schneerson, R.; Liu, T.-Y.; Schiffer, M. S.; Schiffman, G.; Myerowitz, R. L.; McCrackin, G. H., Jr.; Ørskov, I.; Ørskov, F. *The Immune System and Infectious Diseases*; Krager, Basel, New York, 1975; pp 218−241.

10.1021/ja0210087 CCC: $25.00

polysaccharide is due to its similarity to a self-antigen. A protein conjugate of the K92 polysaccharide, however, has resulted in antibodies which react against both the Group B and C meningococcal polysaccharides;[14] the functional significance of these antibodies is not known. The capsular polysaccharide of the *E. coli* K1 serotype, like that of Group B meningococci, is an α(2→8)-linked sialic acid homopolymer;[15] O-acetylated and non-O-acetylated variants of the K1 polysaccharide exist.[16] The *E. coli* K1 organism is the cause of neonatal meningitis.[17]

Because of its similarity to self-antigens, the potential for a vaccine directed against the Group B polysaccharide eliciting autoimmune disease does exist;[1,2] arguments have been presented that this happenstance is not likely.[13] However, data that satisfactorily resolve this issue, especially as it might apply to infants and small children, do not yet exist.

Antibodies against the Group B polysaccharide are found in human sera and can be induced by disease or vaccination with noncovalent complexes;[18−21] however, these antibodies are predominately IgM and of low avidity. They are also unusual in that they do not recognize, or recognize very poorly, α(2→8)-linked sialic acid oligomers with a degree of polymerization (DP) less than ca. 15 residues (DP ≤ 15). Antibodies directed against the polysaccharide generally "recognize" short oligosaccharide domains, including dimers and trimers.[22,23] Jennings and co-workers[24−26] have attributed this behavior, i.e., that antibodies raised against the Group B polysaccharide bind poorly to short Group B oligosaccharides, to the formation of a size-dependent "conformational epitope" within the Group B polysaccharide, and a subsequent antibody response to the epitope. To the extent that conformational epitopes are formed by the Group B meningococcal polysaccharide, and that sialic acid oligomers of N-CAMs and other macromolecules do not form such epitopes, a vaccine directed against the Group B polysaccharide should be both bactericidal and safe.

The need for a Group B meningococcal vaccine, along with the hypothesized importance of secondary structure on the immune response to the Group B polysaccharide antigen, has served as the impetus for a number of structural and conformational studies of the Group B polysaccharide.[27−34] The studies have relied primarily on nuclear magnetic resonance (NMR) spectroscopy, especially the use of scalar coupling constants and nuclear Overhauser effect (NOE) enhancements, although other methods[33] have been used. Several helical conformations have been proposed for the Group B polysaccharide.[26,31] There has been no detailed NMR relaxation time study of the Group B polymer, although such studies could cast considerable light on the potential for the polysaccharide to form a helical epitope. ^{13}C NMR relaxation data for the Group B polysaccharide has been presented by us [27,28] and others;[29] however, these studies were not extensive, and the relaxation times were not analyzed in detail relative to models of polymer motion. We have completed a detailed study of the dynamics of α(2→8)-linked sialic acid polymers in solution as probed by NMR relaxation behavior [T_1, T_2, and NOE (T_1 = $^{13}C-\{^1H\}$ spin−lattice relaxation time; T_2 = $^{13}C-\{^1H\}$ spin−spin relaxation time)] and herein report our results and their implications for a Group B polysaccharide conformational epitope.

Experimental Section

Preparation and Characterization of Polysaccharides. Colominic acid, the α(2→8)-linked sialic acid capsular polysaccharide isolated from *E. coli* serotype K1, was purchased from Calbiochem Biochemicals (San Diego, CA), or isolated from *E. coli* cultures as described.[35] Colominic acid has a ^1H and ^{13}C NMR spectrum identical to that of the Group B meningococcal polysaccharide (data not shown), and was used because it is more readily available. The commercially purchased material was fractionated by size-exclusion chromatography on a 1.6 cm × 100 cm Sephacryl S-300 HR (Pharmacia Biotech, Inc.) column in 100 mM ammonium acetate (pH 7.0), and material with distribution coefficients, K_{av}'s, between 0.10 and 0.56 was collected and combined. This combined fraction is referred to herein as **SA-A**. The absence of oligosaccharides with DP < 20 in the fraction was demonstrated by ion-exchange chromatography (Mono Q HR 5/5 column; Pharmacia Biotech, Inc.)[36] using unfractionated colominic acid and homogeneous preparations of α(2→8)-linked sialic acid dimers, tetramers, and hexamers (E Y Laboratories, Inc., San Mateo, CA) as markers. A high-molecular weight fraction of the K1 polysaccharide, designated as **SA-B**, was isolated on a Sephacryl S-300 HR column using conditions described above; all **SA-B** material had K_{av}'s < 0.10. Both **SA-A** and **SA-B** were analyzed by Superose 6 HR 10/30 (Pharmacia Biotech, Inc.) size-exclusion chromatography in 50 mM NaH_2PO_4 (pH 7.2), 0.2 M NaCl; their molecular weight distributions are markedly distinct (see Figure 2). Aliquots of **SA-A** and **SA-B** were prepared for NMR spectroscopy as deuterium oxide solutions at concentrations of ca. 100 mg/mL in 25 mM NaH_2PO_4 (pD 7.6), with 500 μM ethylenediaminetetraacetic acid added. For these solutions, the measured pH was corrected for the deuterium isotope effect using the relationship pD = pH + 0.4.[37] The solutions were purged with argon gas before NMR analysis to remove dissolved oxygen. Both were found to be stable for months upon storage at 4 °C and showed no signs of degradation. A high-molecular weight fraction of ca. 30% uniformly labeled ^{13}C-labeled *E. coli* K1 polysaccharide was similarly prepared, but at a 10 mg/mL concentration. The ^{13}C-enriched sample was used to evaluate the influence of concentration and viscosity on NMR relaxation of the Group B polysaccharide. Relative viscosities were determined[38] directly

(14) Devi, S. J. N.; Robbins, J. B.; Schneerson, R. *Proc. Natl. Acad. Sci., U.S.A.* **1991**, *88*, 7175−7179.
(15) Jennings, H. J. *Adv. Carbohydr. Biochem.* **1983**, *41*, 155−208.
(16) Ørskov, F.; Sutton, A.; Schneerson, R.; Wenlu, L.; Egan, W.; Moff, G. E.; Robbins, J. B. *J. Exp. Med.* **1979**, *149*, 669−685.
(17) Robbins, J. B.; McCrackin, G. H.; Gotschlich, E. C.; Ørskov, I.; Hanson, L. *New Eng. J. Med.* **1974**, *290*, 1216−1220.
(18) Mandrell, R. E.; Zollinger, W. D. *J. Immunol.* **1982**, *129*, 2172−2177.
(19) Zollinger, W. D.; Mandrell, R. E.; Griffiss, J. M.; Alteri, P.; Berman, S. *J. Clin. Invest.* **1979**, *63*, 836−848.
(20) Lifely, M. R.; Roberts, S. C.; Griffiss, J. M. *Vaccine* **1991**, *9*, 60−66.
(21) Leinonem, L.; Frasch, C. E. *Infect. Immunol.* **1982**, *38*, 1203−1207.
(22) Kabat, E. A. *J. Immunol.* **1960**, *84*, 82−85.
(23) Kabat, E. A. *Structural Concepts in Immunology and Immunochemistry*, 2nd ed.; Holt, Rineheart and Winston, New York, 1976; pp 119−136.
(24) Jennings, H. J.; Katzenellenbogen, E.; Lugowski, C.; Michon, F.; Roy, R.; Kasper, D. L. *Pure Appl. Chem.* **1984**, *56*, 893−905.
(25) Jennings, H. J.; Roy, R.; Michon, F. *J. Immunol.* **1985**, *134*, 2651−2657.
(26) Brisson, J.-R.; Baumann, H.; Imberty, A.; Perez, S.; Jennings, H. J. *Biochemistry* **1992**, *31*, 4996−5004.
(27) Egan, W. *Magnetic Resonance in Biology*; John Wiley and Sons: New York, 1980; Vol. 1, pp 197−258.
(28) Egan, W.; Ferretti, J. A.; Marshall, G. R. *Bull. Magn. Reson.* **1981**, *2*, 15−17.
(29) Lindon, J, C.; Vinter, J. G.; Lifely, M. R.; Moreno, C. *Carbohydr. Res.* **1984**, *133*, 59−74.
(30) Michon, F.; Brisson, J.-R.; Jennings, H. J. *Biochemistry* **1987**, *26*, 8399−8405.
(31) Yamasaki, R.; Bacon, B. *Biochemistry* **1991**, *30*, 851−857.
(32) Baumann, H.; Brisson, J.-R.; Michon, F.; Pon, R.; Jennings, H. J. *Biochemistry* **1993**, *32*, 4007−4013.
(33) Bystricky, S.; Pavliak, V.; Szu, S. C. *Biophys. Chem.* **1997**, *63*, 147−152.
(34) Venable, R. M.; Bizik, F.; Henderson, T. J.; Egan, W. *J. Mol. Struct. (THEOCHEM)* **1997**, *395−396*, 375−388.
(35) Freese, S. J.; Vann, W. F. *Methods Enzymol.* **1993**, *235*, 304−311.
(36) Hallenbeck, P. C.; Yu, P.; Troy, F. A. *Anal. Biochem.* **1987**, *161*, 181−186.
(37) Bates, R. G. *Determination of pH: Theory and Practice*; John Wiley and Sons: New York, 1964; pp 219−220.
(38) Shoemaker, D. P.; Garland, G. W. *Experiments in Physical Chemistry*, 2nd ed.; McGraw-Hill: New York, 1971.

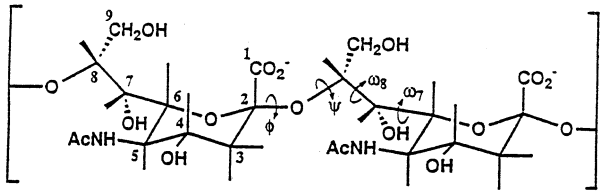

Figure 1. Structure of an α(2→8)-linked sialic acid disaccharide illustrating the four torsion angles defining linkage conformation.

from the measured flow times for 1 mL of the K1 polysaccharide at 10 and 100 mg/mL, using an Ubbelohde microviscometer (Schott-Geräte, GbmH) submerged in a constant-temperature water bath at 25 °C. Reported viscosities are derived from the average of five measured flow times.

NMR Spectroscopy. Natural abundance ^{13}C NMR experiments were conducted on nonspinning samples at 25 °C with a General Electric, Inc. (Freemont, CA) GN-300 spectrometer operating at 75.47 MHz and a Bruker Instruments, Inc. (Billerica, MA) AMX 500 spectrometer operating at 125.77 MHz. All experiments incorporated broad-band proton noise decoupling. T_1 measurements were based on the inversion recovery pulse sequence[39] [180° − τ − 90°-acquisition] with 8−11 randomized τ delays. T_2 measurements used the Carr−Purcell−Meiboom−Gill sequence[39] [90_x° − (τ − 180_y° − τ)$_n$ − acquisition] with τ delays of 2 ms for accumulating 11 different free induction decay (FID) signals, each having a unique value for *n*. Steady state NOE enhancements were evaluated as the difference of two spectra, one acquired with proton noise decoupling applied throughout the entire experiment and the other, with decoupling applied only during acquisition of the FID signal (inverse-gated decoupling). Data sets of 16384 or 32768 complex points and 200 ppm spectral windows were obtained from the accumulation of 8000 (125.77 MHz) or 20000 (75.47 MHz) FID signals, with relaxation delays of at least five (T_1 and T_2 measurements) or 10 (NOE measurements) times the longest protonated carbon nucleus T_1 value. The data sets were transferred to Irix (Silicon Graphics, Inc., Mountain View, CA) computer workstations, where FELIX (Accelrys, Inc., San Diego, CA) software was used to process data sets into spectra. FID data sets were zero-filled (1×) and apodized with a line broadening factor of 5 Hz before Fourier transformation into spectra and phase correction into pure absorption mode. T_1 and T_2 values were derived from fitting spectral signal intensities as a function of τ or 2τ, respectively, to single-exponential expressions.[39]

Computer Modeling. All molecular modeling was performed on Hewlett-Packard (Palo Alto, CA) 9000/700 series workstations using CHARMm[40] software. For the construction of sialic acid polysaccharides, α-sialic acid residues were built from the X-ray coordinates of β-sialic acid dihydrate[41] by inverting the configuration at its anomeric carbon atom. Polysaccharides were built to various degrees of polymerization by concatenating residues together with (2→8) linkages (see Figure 1), as described.[34] The polysaccharides were placed into helical conformations proposed by Yamasaki and Bacon[31] by fixing the C2−O8 bond length at 1.40 Å, the glycosidic bond angle (C2−O8−C8) to 117°, and finally setting the four torsion angles constituting the linkage groups. The ω_7 torsion angle (O6−C6−C7−O7) was set at 60°, and the remaining angles were set to define one of two Yamasaki and Bacon conformations, designated helix A and helix B. For the helix A conformation, ω_8 (O7−C7−C8−O8) was fixed at 60°, ϕ (O6−C2−O2−C8) at 0°, and ψ (C2−O2−C8−C7) at 175.° Corresponding angles for the helix B conformation were −60°, 120°, and 115,° respectively.

Expected rotational correlation times for sialic acid helices of DP = 8, 16, 24, 32, and 40 were computationally estimated using the hydrodynamic bead formalism of de la Torre and Bloomfield,[42] as modified by Venable and Pastor.[43] The helices were modified by deleting all carbon and hydrogen atoms to considerably reduce computation time. The remaining oxygen and nitrogen atoms, comprising the major portion of the solvent accessible surface area, were represented by identical hard spheres or beads. Bead radii were established using a sucrose bead model of only oxygen atoms. Bead radius was adjusted until the experimentally determined translational diffusion coefficient at 20 °C[44] and the rotational diffusion coefficient at 32 °C[45] was reproduced for sucrose in water; bead radii of 2.3−2.6 Å were thus determined. To represent experimental conditions, the hydrodynamic calculations assumed a temperature of 25 °C, and used the Rotne and Prager[46] hydrodynamic interaction tensor with stick boundary conditions to represent water solvent.

Data Interpretation with Rigid Rotor Models and Distributions of Correlation Times. Models of rigid molecule tumbling, as well as statistical distributions of correlation times, were evaluated for their ability to reproduce the observed relaxation times and NOE enhancements. The models and distributions were least-squares fit to the measured T_1, T_2, and NOE values by adjusting their characteristic correlation times using MLAB (Civilized Software Inc., Silver Spring, MD) software on Irix computer workstations. Expressions relating T_1, T_2, and NOE values to these correlation times may be found in refs 48−50. The relaxation of a $^{13}C-^{1}H$ (C−H) vector of a rigid helix is physically characterized by correlation times for rotation along the major and minor axes of the helix, τ_z and τ_x, respectively, and the angle, β, between the C−H bond and the helix major axis. Values for β were calculated for the various C−H vectors on carbon atoms C3 through C9 for the A and B helices (see Table 2). Using these values, τ_x and τ_z were adjusted to fit the T_1, T_2, and NOE values measured for these nuclei at both magnetic field strengths. Random coil motions were represented with two different distributions of correlation times; rectangular distributions,[49] characterized by correlation times τ_a and τ_b (see eq 2), and log − χ^2 distributions,[50] described by a mean correlation time, τ_0, and a width parameter *p* on a logarithmic scale of base *b* (see eqs 3, 4, and 5). The values for τ_a and τ_b, or τ_0 and *p* with *b* held constant at 10, were adjusted to fit the T_1, T_2, and NOE measurements. All curve-fits were repeated several times using different initial values for the correlation times or width parameters to ensure that their final, derived values represented the global minimum value of the sum-of-squares surface.

Results and Discussion

Evaluation of Molecular Dynamics for Low-Molecular Weight α(2→8)-Linked Sialic Acid Polysaccharides. Relaxation Measurements. Commercially purchased colominic acid was fractionated by size-exclusion chromatography to remove material with low degrees of polymerization. A chromatogram of this isolated fraction, referred to as **SA-A**, is shown in Figure 2. (**SA-A** is distinguishable from the faster-eluting **SA-B** fraction; see the Experimental Section.) Troy and co-workers[36] have shown that sialic acid oligomers with chain lengths of up to about DP = 20 may be separated chromatographically; using their method and reference materials of known chain length,

(39) Farrar, T. C.; Becker, E. D. *Pulse and Fourier Transform NMR*; Academic Press: New York, 1967; pp 278−286.
(40) Brooks, B. R.; Bruccoleri, R. E.; Olafson, B. D.; States, D. J.; Swaminathan, S.; Karplus, M. *J. Comput. Chem.* **1983**, *4*, 187−217.
(41) Flippen, J. L. *Acta Crystallogr., Sect. B* **1973**, *29*, 1881−1886.
(42) de la Torre, J. G.; Bloomfield, V. A. *Quart. Rev. Biophys.* **1981**, *14*, 81−139.
(43) Venable, R. M.; Pastor, R. W. *Biopolymers* **1988**, *27*, 1001−1014.
(44) van Holde, K. E. *Physical Biochemistry*, 2nd ed.; Prentice Hall, Inc., Englewood Cliffs, NJ, 1985; pp 99−103.
(45) Kovacs, H.; Bagley, S.; Kowalewski, J. *J. Magn. Reson.* **1989**, *85*, 530−541.
(46) Rotne, J.; Prager, S. *J. Chem. Phys.* **1969**, *50*, 4831−4837.
(47) Heatley, F. *Prog. Nucl. Magn. Reson. Spectrosc.* **1979**, *13*, 47−85.
(48) Woessner, D. E. *J. Chem. Phys.* **1962**, *36*, 1−4.
(49) McCall, D, W.; Douglass, D. C.; Anderson, E. W. *J. Chem. Phys.* **1959**, *30*, 1272−1275.
(50) Schaefer, J. *Macromolecules* **1973**, *6*, 882−888.

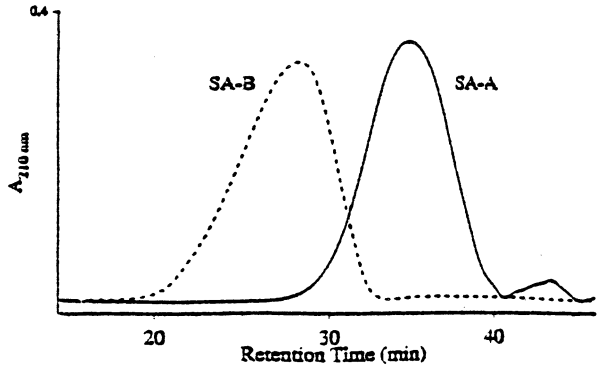

Figure 2. Superose 6 size-exclusion chromatography of **SA-A** and **SA-B**.

Table 1. NT_1, NT_2, and NOE Measurements for **SA-A** and **SA-B**

	75 MHz			126 MHz		
carbon atom	NT_1[a] (ms)	NT_2[a] (ms)	NOE[b]	NT_1[a] (ms)	NT_2[a] (ms)	NOE[b]
			SA-A			
3	201 ± 6	51 ± 7	0.48 ± 0.02	249 ± 23	80 ± 11	0.40 ± 0.04
4	207 ± 1	66 ± 2	0.51 ± 0.04	304 ± 9	76 ± 6	0.45 ± 0.07
5	196 ± 3	57 ± 1	0.50 ± 0.03	256 ± 23	76 ± 12	0.41 ± 0.07
6	202 ± 1	59 ± 1	0.44 ± 0.02	312 ± 5	67 ± 6	0.40 ± 0.10
7	207 ± 3	49 ± 2	0.42 ± 0.00	310 ± 14	56 ± 5	0.42 ± 0.20
8	201 ± 3	49 ± 2	0.46 ± 0.03	310 ± 8	62 ± 5	0.38 ± 0.02
9	202 ± 3	85 ± 5	0.70 ± 0.00	267 ± 13	103 ± 7	0.49 ± 0.20
			SA-B			
3	197 ± 10	44 ± 8	0.55 ± 0.04	205 ± 51	93 ± 8	0.31 ± 0.15
4	218 ± 8	42 ± 2	0.61 ± 0.05	231 ± 27	84 ± 10	0.55 ± 0.20
5	186 ± 7	40 ± 2	0.62 ± 0.03	188 ± 31	95 ± 11	0.30 ± 0.16
6	195 ± 7	40 ± 1	0.52 ± 0.02	246 ± 23	77 ± 8	0.44 ± 0.09
7	196 ± 11	38 ± 4	0.47 ± 0.02	233 ± 25	71 ± 6	0.61 ± 0.05
8	198 ± 14	39 ± 3	0.44 ± 0.04	248 ± 16	76 ± 6	0.40 ± 0.07
9	206 ± 9	61 ± 10	0.76 ± 0.02	246 ± 23	119 ± 13	0.33 ± 0.11

[a] Values are reported with their 95% confidence intervals. [b] Values are an average of three independent measurements reported with their 95% confidence intervals.

we have verified that oligomers shorter than DP = 20 have been successfully removed from **SA-A** (data not shown). An upper value for chain length was not definitively established, however, assuming that K_{av} is approximately a linear function of the logarithm of molecular weight, the majority of the fraction (>95%) had a DP < 200, with a probable mean chain length of about DP = 40.

For **SA-A** material, the $^{13}C-\{^1H\}$ relaxation times NT_1 and NT_2, as well as $^{13}C-\{^1H\}$ steady-state NOE enhancements, were measured for carbon nuclei C3 through C9 at both 7.06 and 11.75 T. The ^{13}C Larmor frequencies corresponding to these magnetic field strengths were ca. 75 and 126 MHz, respectively. The measurements are reported in Table 1 along with their 95% confidence intervals. (Measurements for **SA-B** are also listed in the table.) Additionally, the relaxation behavior for C3 and C4 at 75 MHz, and C5 and C6 at 126 MHz, are shown in Figure 3. The relaxation curves span the entire range of "quality-of-fit" to single-exponential equations. Both spin−lattice and spin−spin relaxation, therefore, are accurately described with single-exponential expressions for all carbon nuclei evaluated.

Although it is reasonable to assume that the nuclear magnetic relaxation of protonated carbon nuclei will be dominated by the dipolar mechanism, relaxation through chemical shift anisotropy (CSA),[51] especially at 11.75 T, should be considered as a possible contributing mechanism. CSA values for the various carbon nuclei of sialic acids in solution have recently been measured to be in the range of 10−17 ppm.[52] When assuming isotropic rotational reorientation and a 11.75 T magnetic field, substitution of the highest value for shift anisotropy into expressions for NT_1(CSA) and NT_2(CSA) reveals that the CSA mechanism contributes less than 1% to the carbon nuclei relaxation rates for any particular correlation time. An isotropic rotor was used only for computational simplicity, and the conclusion that carbon nuclear magnetic relaxation is dominated by the dipolar mechanism will be considered valid for the more complex dynamics below.

Modeling of Rigid Conformations: Isotropic Rotor. The experimental relaxation times and NOE enhancements were initially considered in terms of a model for overall isotropic reorientation (expressions for NT_1, NT_2, and NOE for an isotropic rotor may be found in ref 47). In short, when the NT_1, NT_2, and NOE values of **SA-A** were considered collectively, they were not indicative of isotropically reorienting C−H relaxation vectors. The NT_2 and NOE values measured at 75 MHz, for instance, are not those predicted for an isotropic rotor having NT_1 values of ca. 200 ms (see Table 1). This is illustrated for several of the carbon nuclei in Figure 4, where the correlation times associated with the relaxation data are also given. The data do not yield a single correlation time as they would if a model of simple, isotropic rotation was sufficient to describe the NMR measurements. Very similar inconsistencies are also shown for the data measured at 126 MHz (cf. Figure 4). In addition, some of the experimental relaxation times and NOE enhancements reveal a dependence on magnetic field strength that cannot be explained with the isotropic rotor model; see the correlation times for the NT_2 measurements of C6 (Figure 4) for example. Clearly, a more complex model of molecular dynamics is mandated.

Modeling of Rigid Conformations: Helices. Our next effort was to consider the **SA-A** measurements as arising from the rotational reorientation of a rigid prolate ellipsoid, using the symmetric-top rotor equation developed by Woessner.[48] The prolate ellipsoid is often used as an approximation to a helix; the feasibility and reasonableness of this has been discussed elsewhere.[53,54] The rotational behavior of a C−H relaxation vector on a rigid ellipsoid is characterized by two correlation times, τ_z, about the ellipsoid long axis, and τ_x, about an axis perpendicular to τ_z, and an angle, β, formed by the intersection of the C−H vector and the long axis of the helix. Values of β are explicitly defined by a particular helical conformation; once they are determined for a particular symmetric-top molecule, all that remains is to simply fit, in the least-squares sense, the two correlation times to the NMR data.

Two helical conformations presented in the literature[31] (designated as helix A and helix B; see the computer modeling described in the Experimental Section) were analyzed; β values for their various C−H vectors are listed in Table 2. NT_1, NT_2, and NOE values calculated from the derived helix correlation times are presented graphically in Figure 5 for four **SA-A** carbon nuclei, along with their respective experimental values. As with

(51) Wasylishen, R. E. *NMR Spectroscopy Techniques*; Marcel Dekker: New York, 1987; pp 45−91.

(52) Batta, G.; Gervay, J. *J. Am. Chem. Soc.* **1995**, *117*, 368−374.
(53) Torchia, D. A.; Lyerla, J. A., Jr.; Quattrone, A. J. *Biochemistry* **1975**, *14*, 887−900.
(54) Schleich, T.; Morgan, C. F.; and Caines, G. H. *Methods Enzymol.* **1989**, *176*, 386-418.

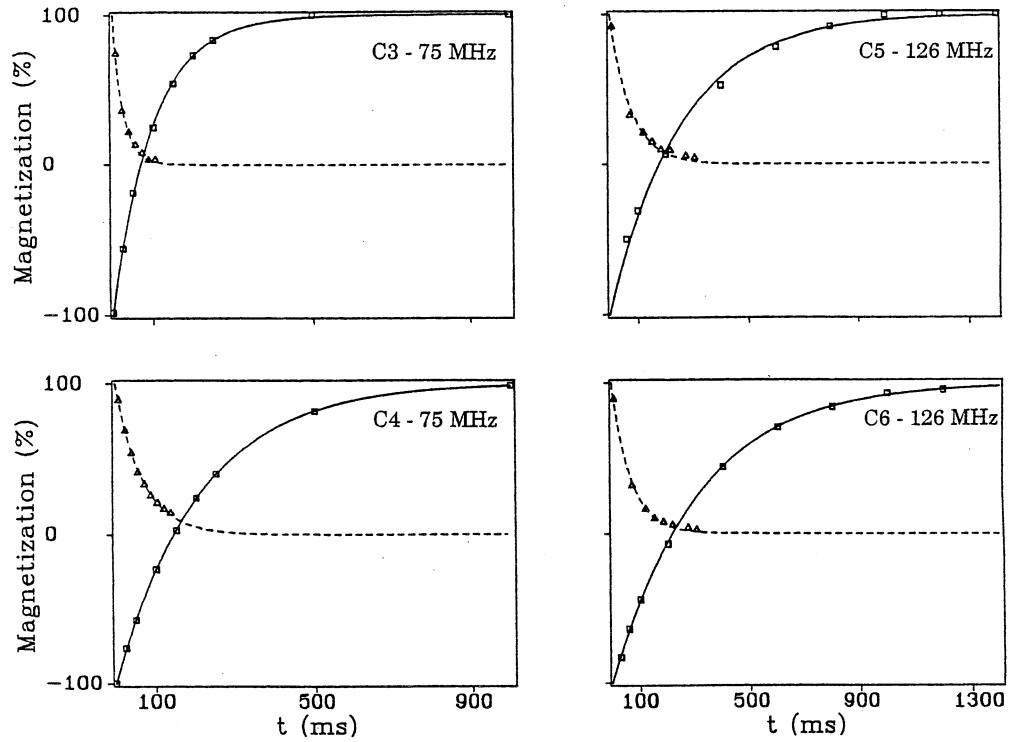

Figure 3. **SA-A** Measurements of bulk magnetization along the *z* axis (the direction of the static magnetic field) following inversion with a 180° pulse (□), and in the *x*−*y* plane (perpendicular to the static field) following a 90° pulse (△), both as a function of time (*t*). Recovery of bulk magnetization along the *z* axis (—) and its decay in the *x*−*y* plane (- - -), calculated from derived T_1 and T_2 values, respectively, are also shown.

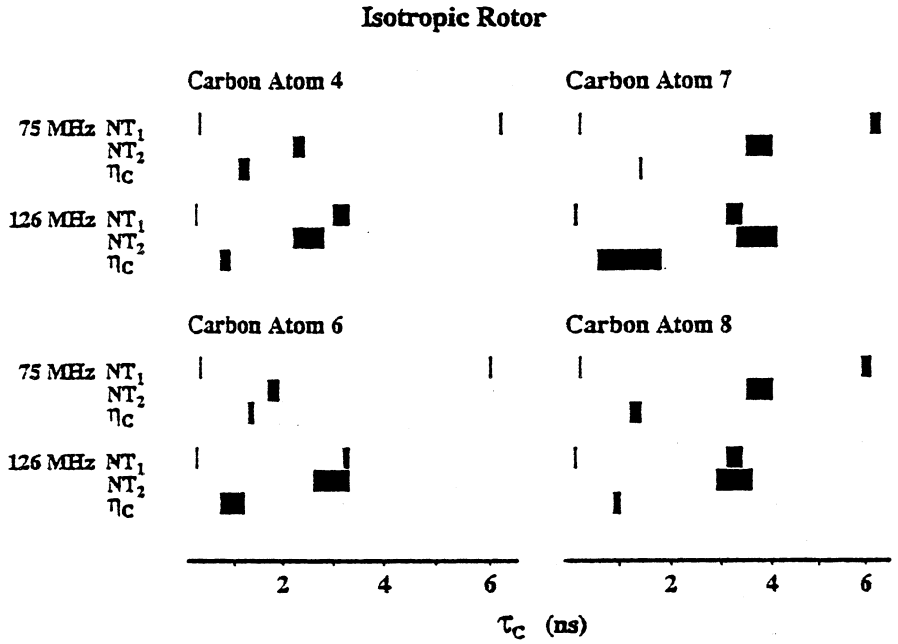

Figure 4. Isotropic rotor correlation times (τ_c) derived from the 95% confidence intervals of the NT_1, NT_2, and NOE (η_c) values measured at 75 and 126 MHz for **SA-A** nuclei C4, C6, C7, and C8. In this presentation, the isotropic rotor model successfully accounts for Table 1 measurements only when all NT_2 and NOE data bars, and one NT_1 data bar at each magnetic field strength for every carbon nucleus, fall above a single correlation time. Data bars progressively scatter as the model becomes increasingly less successful at accounting for the measurements.

the isotropic rotor model, a satisfactory, self-consistent fit of the data to the correlation times was not possible for either conformation. At 75 or 126 MHz for example, when NT_2 and NOE values were used to obtain a set of correlation times, the NT_1 values calculated from them were discordant with the experimental values. Moreover, the correlation times found to best account for the relaxation data obtained at one magnetic field strength were not very predictive of the relaxation behavior observed at the other.

The best fit of the experimental data to the overall tumbling of the helical conformations provided correlation times, τ_x and τ_z, in the ranges of 3−10 ns and 1−2 ns, respectively (cf. Table 3). The relevance of these correlation times can be evaluated by comparison to values derived from hydrodynamic modeling

Table 2. β Values for α(2→8)-Linked Sialic Acid Octamer Helices[a]

carbon atom	β (deg) helix A	helix B
3	55.0[b]	56.4[b]
4	32.7	60.1
5	34.0	59.1
6	31.4	57.5
7	61.5	72.4
8	30.1	52.0
9	57.0[b]	63.0[b]

[a] Helical conformations described by Yamasaki and Bacon.[31] [b] Average of two β values, one for each C−H bond of the chemical group.

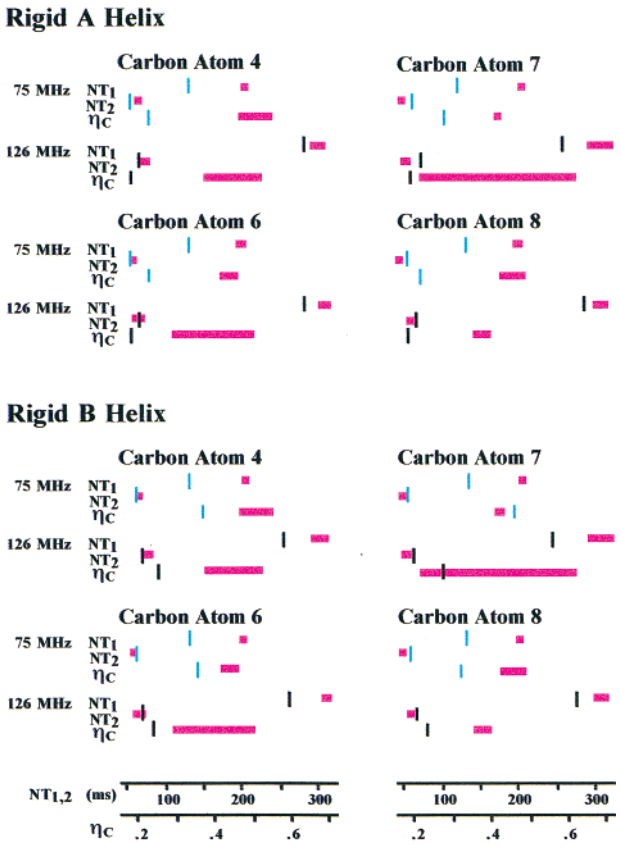

Figure 5. Relaxation times and NOE enhancements predicted from the rotational correlation times derived from modeling the overall rotational reorientation of the helix A and helix B conformations.[31] The predicted NT_1, NT_2, and NOE (η_c) values for 75 MHz, calculated from τ_x and τ_z derived from the 126 MHz measurements (vertical blue lines), and the corresponding values for 126 MHz derived from the 75 MHz measurements (vertical black lines), are shown for **SA-A** nuclei C4, C6, C7, and C8. The 95% confidence intervals for the corresponding measurements from Table 1 (red horizontal bars) are also shown. For these presentations, a rigid helical conformation successfully accounts for the measurements only when all blue and black lines fall within red horizontal bars. Distances separating the blue or black lines from their respective red bars increase as a rigid conformation becomes less successful at accounting for the measurements.

of the helices. A modified version[43] of the hydrodynamic bead formalism described by de la Torre and Bloomfield[42] was used to calculate τ_x and τ_z for the rotational reorientation of sialic acid helices of various lengths. Bead radii of both 2.3 and 2.6 Å were used, giving virtually identical results in calculations of helix rotational correlation times. Values for τ_x and τ_z were calculated for α(2→8)-linked sialic acids of DP = 8, 16, 24, 32, and 40 in rigid helix A and helix B conformations. Correlation times for helix A conformations are shown in Figure 6 as a function of chain length. Because the A and B

Table 3. Rotational Correlation Times Derived from Modeling **SA-A** and **SA-B** Measurements in Terms of Overall Helix[a] Reorientation

sialic acid fraction	helix A τ_x (ns)	helix A τ_z (ns)	helix B τ_x (ns)	helix B τ_z (ns)
SA-A	3.2	2.1	9.4	0.7
SA-B	2.2	1.8	9.2	0.7

[a] Helical conformations described by Yamasaki and Bacon.[31]

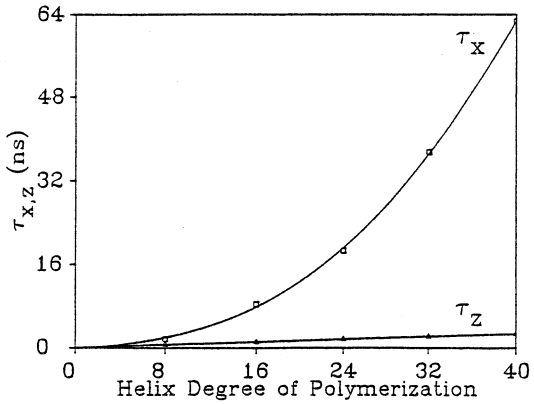

Figure 6. τ_x and τ_z values calculated for rigid α(2→8)-linked sialic acid helices as a function of chain length. τ_x and τ_z values were explicitly calculated for unhydrated helix A[31] models of DP = 8, 16, 24, 32, and 40.

conformations are nearly identical in translational distance per residue and helix diameter, the hydrodynamic behavior of the rigid B helix is virtually identical to that shown for helix A. The τ_x value for helix A deriving from the NMR measurements is approximately 3.2 ns, and as seen in Figure 6, the value corresponds to a helix with a DP = 10−11, clearly inconsistent with established chain lengths for **SA-A** (vide supra). The τ_z values (ca. 0.8 ns) for the A helix derived from the bead model are, as expected, relatively independent of length; they are slightly shorter than the experimentally derived values (ca. 2 ns). This discrepancy may be due to the hydration of the sialic acid polymer in solution, which is not considered in the current hydrodynamic modeling. The introduction of hydration would, however, simply lower the chain length required to fit the experimental data. DP = 10−11 therefore, corresponds to an upper limit for the helix length that would agree with the NMR-derived correlation times. A similar analysis can be conducted for the B helix. The τ_x value derived from the NMR data was 9.4 ns, corresponding to a helix with a DP = 17−18, far short of the average chain length of the **SA-A** polysaccharides estimated at DP = 40. Again, because hydration was not considered, this constitutes an upper limit. Therefore, it is evident that these helices, at least as rigid conformations, are not appropriate for interpreting the experimental results.

Modeling of Flexible Conformations: Helices with Internal Motion. The Woessner equation can be modified to include the affects of internal motion. This provides a means to consider nuclear magnetic relaxation in terms of a "flexible helix," a helical conformation undergoing some degree of internal motion, but not enough to compromise helical topology. The model has been previously applied to DNA helices.[55] A single parameter,

(55) Withka, J. M.; Swaminathan, S.; Bolton, P. *Computational Aspects of the Study of Biological Macromolecules by Nuclear Magnetic Resonance Spectroscopy*; Plenum Press: New York, 1991; pp 409−420.

an effective correlation time, τ_{eff}, represents overall rotational reorientation (τ_x and τ_z) together with the internal diffusion of the C−H relaxation vector in an ellipsoidal cone. The τ_{eff} expression derived by Withka et al.[55] is presented below:

$$\tau_{eff} = \frac{\frac{1}{4} + \frac{3\cos(2\beta)}{2\exp(2\theta^2)} + \frac{9 + 9\cos(4\beta)}{8\exp(4\theta^2)}}{4\tau_x^{-1}} + \frac{9\left[1 + \frac{1}{2\exp(4\theta^2)} - \frac{2\cos(2\beta)}{\exp(2\theta^2)} + \frac{\cos(4\beta)\exp(-4\theta^2 - 4\epsilon^2)}{2}\right]}{16(\tau_x^{-1} + 2\tau_z^{-1})} + \frac{9[\exp(4\theta^2) - \exp(-4\theta^2 - \epsilon^2)\cos(4\beta)]}{4(5\tau_x^{-1} + \tau_z^{-1})} \quad (1)$$

In this equation, θ is the square root of the mean square polar angle of motion, ϵ, the square root of the mean square azimuthal angle of motion, and β, τ_x and τ_z are defined as above. In the absence of internal motions ($\theta = \epsilon = 0°$), this expression reduces to Woessner's equation. The affects of internal motion incorporated into the A and B conformations have been examined within the framework of this equation. Using τ_x and τ_z values for longer helices (25 residues or more) in the hydrodynamic modeling (see Figure 6), and β values for the A or B conformations (Table 2), increasing degrees of internal motion may be added (increasing θ and ϵ) until the effective correlation times agree with those deriving from the NMR data (Table 3). Proceeding in this manner, a 25-residue B helix requires substantial internal motion ($\theta = \epsilon = 30°$) to model as the 18-residue helix derived from the measurements. Considering that θ and ϵ are half-cone angles, this corresponds to a very nonrigid, or flexible helix (when $\theta = \epsilon = 45°$, the model returns to an isotropic rotor). Moreover, recognizing that the majority of polysaccharide chains are substantially longer than 25 residues (vide supra), it becomes apparent that simply adding internal motions into a rigid helix B conformation will not result in an agreement with experiment. Additionally, because the A helix modeled as having a smaller DP, it also cannot be reasonably modeled as a flexible helix with a DP greater than 25. When incorporating extreme amounts of internal motions, the model once again fails to explain the **SA-A** measurements.

Random Coil Chains. Our final effort was to assume that the contribution of overall molecular tumbling on nuclear magnetic relaxation is insignificant and to consider the **SA-A** data in terms of random coil polysaccharide chains. The dynamics of random coil chains can be overwhelming and encompass far too many internal motions to be characterized by one[56] or two[57] correlation times. In addition, because these motions are largely unknown, motional models are typically not available for data interpretation. However, statistical distributions of correlation times can provide an empirical means to describe these dynamics.[47,56] The dynamic range of random coil motional frequencies is often large, differing by several orders of magnitude, and are usually described on a logarithmic scale. Although many such distributions have been reported, perhaps the simplest is the rectangular distribution proposed by McCall and co-workers.[49] Two correlation times, τ_a and τ_b ($\tau_a < \tau_b$), define the boundaries of a continuous, equally weighted distribution. The spectral density function, $J(\omega)$, for a rectangular distribution of correlation times is presented below:

$$J(\omega) = \left[\frac{2}{\omega \ln\left(\frac{\tau_b}{\tau_a}\right)}\right] \tan^{-1}\left[\frac{\omega(\tau_b - \tau_a)}{1 + \omega^2\tau_a\tau_b}\right] \quad (2)$$

Table 4. NT_1, NT_2, and NOE Values Calculated from Rectangular Distributions of Correlation Times Derived from **SA-A** and **SA-B** Measurements

		75 MHz			126 MHz		
carbon atom(s)	$\tau_a - \tau_b$ (ns)	NT_1 (ms)	NT_2 (ms)	NOE	NT_1 (ms)	NT_2 (ms)	NOE
			SA-A				
3−6	0.33−12.61	174	60	0.53	317	67	0.40
7−8	0.30−16.81	183	52	0.55	335	57	0.42
9	0.24−6.50	162	88	0.64	279	104	0.49
			SA-B				
3−6	0.35−12.60	173	59	0.52	318	66	0.39
7−8	0.32−14.96	179	55	0.54	328	61	0.41
9	0.32−5.11	154	91	0.60	266	111	0.43

To consider **SA-A** as a population of random coil chains, its NT_1, NT_2, and NOE measurements were evaluated in terms of the spectral density function above. Because pyranose ring atoms can be expected to experience different types of internal motions than linkage group atoms, C3−C6 were considered separately from the three linkage group atoms when fitting the measurements to the rectangular distributions. Further, as it may be somewhat unrestrained from free rotation,[34] the C9 pendant group was considered separately from all other atoms. Initially, the NT_1, NT_2, and NOE measurements at both magnetic field strengths were plotted as functions of τ_a, with τ_b held constant at different, estimated values. Changes in τ_a were found to significantly affect the NT_2 and NOE values, while the NT_1 plots were virtually unchanging. Similar plots generated as a function of τ_b, with estimated τ_a values held constant, illustrated that changing τ_b values significantly influenced NT_1 and NT_2 values only. Therefore, the NT_2 measurements at 75 and 126 MHz were used in initial least-squares fits to the distributions of correlation times to provide starting values for τ_a and τ_b, then both NT_1 and NOE measurements were added to arrive at the final τ_a and τ_b values. These final values appear in Table 4, with their calculated NT_1, NT_2, and NOE values for both magnetic field strengths. Comparison of these values with experiment (Table 1), reveals that the NMR measurements are explained reasonably well in terms of the distributions. Most all of the **SA-A** measurements (38 of 42 or 91%) for example, differ from their calculated value by less than 20%, and overall agreement between the calculated and experimental **SA-A** values is better than 70%. The distributions derived for the linkage group atoms are very similar to those for the pyranose ring atoms, with the linkage group distributions being only slightly broader. The C9 distribution however, is roughly half as broad as these distributions, and encompasses only their faster correlation times.

Because correlation times described by rectangular distributions are weighted equally, it can be argued that they are not realistic representations of random coil motions. In particular,

(56) Connor, T. M. *Trans. Faraday Soc.* **1964**, *60*, 1574−1591.
(57) Schaefer, J.; Natusch, D. F. S. *Macromolecules* **1972**, *5*, 416−426.

Table 5. NT_1, NT_2, and NOE Values Calculated from Log $-\chi^2$ Distributions of Correlation Times Derived from **SA-A** and **SA-B** Measurements[a]

			75 MHz			126 MHz		
carbon atom(s)	*p*	τ_o (ns)	NT_1 (ms)	NT_2 (ms)	NOE	NT_1 (ms)	NT_2 (ms)	NOE
			SA-A					
3−6	6	1.80	165	58	0.55	292	65	0.41
7−8	6	2.24	167	49	0.48	307	54	0.36
9	7	1.14	163	86	0.70	269	101	0.51
			SA-B					
3−6	6	1.80	165	58	0.55	292	65	0.41
7−8	5	2.30	172	41	0.50	314	44	0.38
9	9	1.70	155	72	0.52	276	84	0.36

[a] Distributions derived from NT_1, NT_2, and NOE measurements with *b* fixed at 10.

simple motions involving only a few atoms of a single residue, such as simple rotation about torsion angles, can be expected to occur much more frequently than segmental chain motions involving several or even many residues of a chain. For this reason, descriptions of large numbers of correlation times based on Gaussian or log $-\chi^2$ distributions may be more representative of the motional dynamics of random coil chains.[47,56] The two distributions are similar in that they are defined by a width parameter and a mean (or effective) correlation time. The log $-\chi^2$ distribution however, is highly asymmetric, with a pronounced tail at the long correlation time region of the distribution; the shorter correlation times are weighted more heavily than these long correlation times. Defining a logarithmic scale s,

$$s = \log_b [1 + (b - 1)\tau/\tau_o], \quad (3)$$

where *b* is the logarithmic base, and τ_o, the mean correlation time, a density function *F(s)*,

$$F(s) = \frac{p}{\Gamma(p)} (ps)^{p-1} \exp(-ps) \quad (4)$$

that includes an adjustable width parameter, *p*, and the gamma function, $\Gamma(p)$; *J(ω)* becomes

$$J(\omega) = \int_0^{+\infty} \frac{\tau_0 F(s)(b^s - 1)ds}{(b - 1)\{1 + \omega^2 \tau_0^2[(b^s - 1)/(b - 1)]^2\}} \quad (5)$$

for log $-\chi^2$ distributions of correlation times.[50]

For each rectangular distribution in Table 4, a log $-\chi^2$ distribution of correlation times was found that defined comparable NT_1, NT_2, and NOE values. When deriving the log $-\chi^2$ distributions therefore, *b* was held constant at 10 to define them on the same scale as the rectangular distributions. They are reported as log $-\chi^2$ distributions of correlation times, the final *p* and τ_0 values of which appear in Table 5 with their calculated relaxation times and NOE values. As for the rectangular distributions, the slightly broader distribution observed for linkage group carbon atoms relative to those for the pyranose rings, and the considerably narrower distribution for C9, are all preserved in the log $-\chi^2$ distribution of correlation times.

Evaluation of Molecular Dynamics for High-Molecular Weight α(2→8)-Linked Sialic Acid Polysaccharides. Sample Preparation and NMR Measurements. Evaluation of NMR relaxation times and NOE enhancements for polymers as a function of chain length can provide valuable insight into their dynamic behavior. Relaxation times measured for polymer chains adopting virtually rigid topologies for instance, are expected to reveal a strong dependence on chain length,[47,58] while such dependencies are not expected, or typically observed, for random coil chains.[47] To study the affects of chain length on the nuclear magnetic relaxation of α(2→8)-linked sialic acid polysaccharides, we isolated a second, high-molecular weight fraction of the polysaccharide, referred to as **SA-B**, from the K1 serotype of *E. coli*. On a size-exclusion chromatographic column, this material was distinct from **SA-A** (see Figure 2). We assume that the difference in retention times for the fractions reflects higher degrees of polymerization for the **SA-B** material; moreover, we have surmised that the average DP for the fraction is approximately 400 by assuming that K_{av} is approximately a linear function of the logarithm of molecular weight.

$^{13}C-\{^1H\}$ relaxation times and NOE enhancements measured at 7.06 and 11.75 T for the **SA-B** material are listed in Table 1, together with the experimental **SA-A** data for comparison. To a first approximation, the **SA-B** and **SA-A** data are very similar; no striking differences are apparent between the two fractions. At 75 MHz, the NT_1 values for both fractions are essentially identical, and there are only slight differences between their NT_2 and NOE values. Similar small differences are also observed between the 126 MHz **SA-B** values and their **SA-A** counterparts.

Relaxation times may be influenced by solution viscosity[47] and should be considered when comparing fractions of different degrees of polymerization. For C3, C6, and C9, NT_1 and NOE values were measured at 126 MHz for a much less concentrated (10 mg/mL) ^{13}C-labeled *E. coli* K1 capsular polysaccharide fraction having a distribution of chain lengths similar to that of **SA-B** (data not shown). The viscosities of the two fractions are expected to differ substantially; estimated viscosities for the ^{13}C-labeled faction and **SA-B** are 3 and 23 cSt, respectively. All NT_1 and NOE values measured for the ^{13}C-labeled faction were found to fall within the 95% confidence intervals of their respective **SA-B** value. The differences in viscosity therefore, do not appear to have an appreciable affect on **SA-B** nuclear magnetic relaxation.

Data Interpretation with Rigid and Flexible Conformational Dynamics. In a manner similar to that detailed for **SA-A**, we have attempted to explain the **SA-B** measurements with specific models of molecular dynamics. In short, the small differences observed between the **SA-A** and **SA-B** data were found to have little or no influence on modeling. For the isotropic rotor model, all **SA-B** values define similar or identical rotational correlation times as their corresponding **SA-A** values (Figure 4), and therefore, no single correlation time describing all **SA-B** measurements could be found. When modeling helix A rotational reorientation, the **SA-B** measurements gave "best fit" rotational correlation times very similar to those found when using the **SA-A** data (Table 3), representing sialic acid helices differing in chain length by only a single residue according to hydrodynamic bead formalism (Figure 6). The **SA-B** data defined a 9−10 residue helix, while the corresponding **SA-A** helix was 10−11 residues in length. In the case of helix B

(58) Budd, P. M.; Heatley, F.; Holton, T. J.; Price, C. *J. Chem. Soc., Faraday Trans.* **1981**, *1*, *77*, 759−771.

Table 6. 25 MHz $^{13}C\{^1H\}$ NT_1 Measurements[a] for the α(2→8)-Linked Sialic Acid Polysaccharide and Values Calculated from Rectangular[b] and Log $-\chi^2$ [c] Distributions of Correlation Times

		calculated values (ms)	
carbon atom	measurements (ms)	rectangular distributions	log $-\chi^2$ distributions
3	63	59	62
4	64	59	62
5	67	59	62
6	64	59	62
7	64	60	61
8	70	60	61
9	97	64	60

[a] Measurements are from Egan et al.[28] [b] **SA-B** distributions from Table 4. [c] **SA-B** distributions from Table 5.

rotational reorientation, the two sets of correlation times were virtually identical and represent sialic acid helices of the same length (DP = 17−18). As found for **SA-A**, these derived helix lengths clearly fall short of being consistent with those shown to exist in the **SA-B** fraction. Further, because **SA-B** is composed of sialic acid chains of a considerably higher degrees of polymerization than **SA-A**, all attempts to rationalize the **SA-B** data by introducing internal motions into helix A and helix B conformations only become more difficult than that described for the **SA-A** data. Once again, only statistical distributions of correlation times could justify the NMR measurements. The rectangular and log $-\chi^2$ distributions derived from the **SA-B** measurements are reported in Tables 4 and 5, respectively, along with those from the **SA-A** data. With the possible exception of the only the C9 log $-\chi^2$ distributions, all **SA-B** distributions are very similar or identical to their **SA-A** counterparts, undoubtedly a reflection of the similarity between their measurements. Finally, 25 MHz NT_1 measurements reported years ago[28] for a high-molecular weight fraction of the *E. coli* K1 capsular polysaccharide are listed in Table 6, with those calculated from the **SA-B** rectangular and log $-\chi^2$ distributions. It is remarkable that with the exception of C9 only, the distributions define 25 MHz NT_1 values very close to those reported previously.

Conformational Flexibility of α(2→8)-Linked Sialic Acid Polysaccharides in Solution. When considering our NMR measurements and interpretations with rigid rotor models, it becomes clear that overall rotational reorientation cannot be a dominant force on the nuclear magnetic relaxation of long (DP > 15), α(2→8)-linked sialic acid polysaccharides in solution. We have conclusively eliminated rigid, isotropic rotors and helix A and B symmetric top rotors as plausible models for polysaccharide solution dynamics. While each model has its specific limitations, they all share a common shortcoming; not one can account for the magnetic field strength dependence of the experimental NT_1 and NT_2 values. This is also the case for our interpretations with "flexible helices," even with extreme internal motion. A simple comparison of the **SA-A** and **SA-B** measurements however, probably gives the most direct evidence for eliminating rigid rotor models altogether; the NT_1, NT_2, and NOE values vary little, and are statistically identical in many cases, while the degree of polymerization varies by about a factor of 10. For all descriptions of rigid rotor dynamics, NT_1, NT_2, and NOE values must change with polymer chain length (see refs 47 and 58 for examples). Internal motions and not molecular tumbling therefore, must provide the dominant force for the nuclear magnetic relaxation of the **SA-A** and **SA-B** polysaccharides, implying that considerable conformational flexibility must accompany long α(2→8)-linked sialic acid polysaccharide chains in solution. Very similar results have been observed for synthetic, random coil polymers, where NMR relaxation measurements become independent of chain length above a specific, critical value.[47] For sufficiently long polymers, relaxation is dominated by local, segmental motions unaffected by the polymer chain length, with the length of this mobile segment dependent upon polymer structure. We conclude therefore, that the Group B meningococcal capsular polysaccharide is a random coil chain in solution.

We have derived distributions of correlation times that reasonably account for our measured relaxation times and NOE enhancements. In comparison to the rigid rotor models, the distributions are far superior at explaining the experimental data, and surprisingly capable of accounting for the magnetic field strength dependence of the measured relaxation times. This is best illustrated by the near perfect prediction of 25MHz NT_1 values[28] for C3−C8, using the distributions derived from our experimental data (Table 6). We have also used these distributions to roughly approximate the shortest length along the α-(2→8)-linked sialic acid polysaccharide chain capable of all dominant motions contributing to nuclear magnetic relaxation. (As discussed above, relaxation times and NOE enhancements should be independent of the polysaccharide DP above this length.) A mean value for each reported distribution, calculated from τ_a and τ_b for rectangular distributions and represented by τ_o for log $-\chi^2$ distributions, was used as τ_{eff} in eq 1, with $\theta = \epsilon = 0°$, to derive values for τ_x and τ_z. The hydrodynamic modeling data (Figure 6) was then used to interpolate a helix A length corresponding to these rotational correlation times. For the pyranose ring log $-\chi^2$ distributions, the mean chain length corresponds to a 22.4 to 30.8 Å rigid segment, or a DP = 8−11, depending upon β angle. When using the linkage group distributions, this segment is between 25.2 and 36.4 Å (DP = 9−13) in length. Segment lengths derived from the rectangular distributions are similar, roughly 36 Å (DP = 13) for both ring and linkage group carbon atoms. Realizing that these are rough approximations, and that specific internal motions are not known, one should hesitate to put much physical significance on the derived lengths.

Inferences concerning the motional processes of α(2→8)-linked sialic acid polysaccharides may be drawn from the derived distributions of correlation times. Their broad nature imply a wide range of internal motions, most likely ranging from fast, local motions of only one or two atoms, such as rotation about torsion angles, to much slower segmental motions involving a number of residues linked in series. The distributions derived for the pyranose rings and linkage groups are very similar in width and time scale, an observation that is somewhat unexpected. Although it seems reasonable to consider the linkage group conformation as flexible, this is generally not the case for pyranose ring systems, especially when considering that structural studies of α(2→8)-linked polysialic acids reveal evidence of only a single, well-defined $^2C_5$ ring conformation.[29,31] The observation may be rationalized best by Lerner

and co-workers,[59] who have concluded that all atomic sites within pyranose ring systems have some degree of motional freedom, most likely in the form of ring librations, which enable them to sample significant conformational space while generally never leaving the constraints of a single, global conformation. Finally, the distributions derived for the C9 pendant groups are consistently narrower than the others and represent faster internal motions as well. It may be that this group is dominated by only a few, or possibly even a single, dynamic process. Preliminary results from our molecular dynamics simulations show the predominant motion of this group to be rotation about the O8−C8−C9−O9 torsion angle.

Conformational Epitope for the Group B Meningococcal Polysaccharide. Several authors have proposed the existence of a conformational epitope for the Group B meningococcal polysaccharide on the basis of interpretations of NMR results. From the measurement of ^{13}C spin−lattice relaxation times at 63.1 and 100.5 MHz, Lindon and co-workers[29] concluded that the polysaccharide tumbles isotropically in solution as a rigid species and suggested that it bears conformational epitopes. Yamasaki and Bacon,[31] from a quantitative analysis of nuclear Overhauser and exchange spectroscopy (NOESY) data with rigid conformers, reported that the polysaccharide exists as an ordered, helical conformation in solution. And more recently, Brisson and co-workers[26] have concluded from NOESY spectra and potential energy calculations that, although predominantly random coil in nature, the polysaccharide adopts local, extended helical conformations, or pseudohelices, that contain antigenic epitopes. The pseudohelices are proposed to be conformers that the polysaccharide chain can assume in solution, and interactions such as hydrogen bonds, that could stabilize them have not been implicated. In this respect, the pseudohelices are not typical of molecules usually described by the flexible helix model, which for instance, has been used to describe DNA helices. Our findings are in sharp contrast to the conclusions of both Lindon and co-workers[29] and Yamasaki and Bacon[31] and, in general, disagree with any rigid structure for the polysaccharide chain. Further, while our findings are consistent with the random coil nature reported for the polysaccharide by Brisson and co-workers,[26] our NMR data and dynamics modeling cannot be used to argue for pseudohelices occurring along the polysaccharide chain. Experimental evidence conclusively demonstrating the existence of these pseudohelices is expected to be very difficult to obtain. Because they are only minor contributors to the total number of conformers possible for the random coil polysaccharide,[26] the contributions of the pseudohelices to relaxation and cross relaxation should be impossible to dissect from measured relaxation times and NOE enhancements. The use of molecular dynamics simulations to interpret NOESY spectra may be the best approach for supplying evidence for these pseudohelices.

The unusual length dependency demonstrated by α(2→8)-linked sialic acid oligomers in their recognition by antibodies raised against the Group B meningococcal polysaccharide has been attributed to the formation of a size-dependent, ordered, conformational epitope for the polysaccharide chain, and subsequent antibody response to the epitope.[24−26,31] Our results reveal that such an epitope cannot be the result of any energetically stable conformer, as previously suggested.[31] For a conformationally flexible antigen, the polysaccharide chain would have to undergo topological rearrangements from a disordered random coil to the more ordered conformer representing the antigenic epitope; the probability of this conformer occurring in any short oligomer can be expected to be low. Further, for oligomers between DP = 10−17, the progressively improved binding found as a function of chain length[25] could be explained by an increasing probability for the occurrence of the conformer representing the epitope. While a minimum oligosaccharide length is a requirement for antigenicity, it also appears that long α(2→8)-linked sialic acid chains can adopt conformers that are found with low probability, or not found at all, in their smaller oligomers. This is consistent with the observation that the linkage groups of α(2→8)-linked sialic acid oligomers between DP = 2−6 differ conformationally from the internal linkage groups of the polysaccharide.[30]

Conclusions

From detailed interpretations of NMR relaxation times and NOE enhancements, we have demonstrated that overall molecular tumbling is not a significant process for the nuclear magnetic relaxation of the Group B meningococcal polysaccharide in solution. This was confirmed experimentally by showing that measured relaxation times and NOE enhancements remain essentially unchanged as polysaccharide chain length varies substantially, and indicates that the polysaccharide chain has considerable conformational flexibility. Statistical distributions of correlation times were derived individually for the linkage groups, pyranose rings and methoxy pendant groups that are capable of explaining all experimental data. The distributions derived for the rings and linkage groups are very similar in width and time scale, implying that the ranges of motional frequencies for these regions are comparable. In contrast, the distributions for the hydroxymethyl groups are much narrower and encompass faster correlation times. The motions of these groups appear to be dominated by substantially fewer dynamic processes. Our results present a strong argument against any epitope based on a rigid conformation for the polysaccharide chain and are consistent with the random coil nature suggested for the polysaccharide in solution.[26]

JA0210087

(59) Hajduk, P. J.; Horita, D. A.; Lerner, L. E. *J. Am. Chem. Soc.* **1993**, *115*, 9196−9210.